

Chapter 7

Evaluating Pulse Simulator Using Fluorescent DIC



Chi-Hung Hwang, Rui-Cian Weng, Yen-Pei Lu, Wei-Chung Wang, Tzu-Yu Kuo, and Chun-Wei Lai

Abstract The artery vessel simulator mimics the pulse using a membrane pump to drive water flow through the PDMS phantom intermittently to simulate the blood flows in the artery vessel. The DIC method performs the evaluation, where the images used for DIC calculation are captured by a single-camera stereo-imaging system, which can eliminate the time synchronization issue. The fluorescent medicine FITC is used to generate the random patterns on the surface of a PDMS phantom, where the PDMS phantom is part of the artery vessel simulator. The DIC method determines the displacement and strain field introduced by the interaction between water and the PDMS phantom to know the mechanical behavior of the simulator. In this study, two different imaging modes are implemented to see the time various mechanical behavior of water-PDMS phantom interaction and the simulator's stability. Some challenges for using FITC to the PDMS would be highlighted at the end of this paper.

Keywords Artery vessel · Simulator · Fluorescence · Digital image correlation

7.1 Introduction

The digital image correlation method (DIC) is used for determining the object deformation or movement by tracking random patterns among images. The random marks either generated artificially or native posed are the must for performing the DIC method. While utilizing the DIC for various applications, the contact force is inevitably generated while rendering artificial random marks on the object surface. Thanks to some adequate methods, such as spraying, the force introduced while generating patterns are considered tiny and ignorable and always regarded as non-contact measurement methods. Nowadays, the DIC is widely used for different objects, such as determining the mechanical behaviors for common mechanical materials, constructing materials, soft materials, biomaterials, and others. One of the DIC practical applications is to determine the mechanical properties of biomaterials. During the last two decades, a tremendous amount of research on applying DICs to biomaterials has been reported, such as determining the mechanical properties of cells by tracking fluorescent particles [1], evaluating the mechanical behaviors of muscles [2–4], and evaluating the ventricular volume change after cardiac surgery [5–7]. This study is part of a project on developing a DIC system for general surgery to detect the possible vessel leakage and the mechanical behaviors of the organ after suture to replace the existing methods such as using radiopharmaceuticals and radiation detectors for vessel leakage detection.

While applying DIC to the in vivo applications, the compound used for generating random marks must be biological toxicity-free, and the system must be adequately evaluated to prove that the system performance meets the requirement, and the system configuration is well developed before either animal tests or clinical trials. Thus, to assess the imaging system design of a DIC system for the possible surgery applications, a simple simulator to simulate the mechanical interaction between the vessel and the tissue above the artery is essential. Therefore, the purpose of this study is to evaluate the artery simulator using DIC stereo-DIC method with the random surface pattern generated by fluorescent medicine before finalizing the system design.

C.-H. Hwang (✉) · R.-C. Weng · Y.-P. Lu
National Applied Research Laboratories, Taiwan Instrument Research Institute, Taipei, Taiwan
e-mail: chhwang@narlabs.org.tw

W.-C. Wang · T.-Y. Kuo · C.-W. Lai
Department of Power Mechanical Engineering, National Tsing Hua University, Hsinchu, Taiwan

7.2 The Experimental Setup and the Artery Simulator [8]

Figure 7.1 shows the experimental setup used in this study, consisting of a single camera stereo-DIC imaging system and an artery simulator. In this study, FITC (fluorescein isothiocyanate) is adopted to generate the artificial random pattern on the object surface. FITC can be excited at a peak wavelength around 495 nm and emits light at the peak wavelength of 519 nm. A self-made LED light source with the center wavelength around 475 nm is implemented to excite the FITC, and a long-pass filter with a cut-on frequency at 500 nm is placed in front of the lens for blocking the excitation light. A signal camera stereo-imaging optical imaging system is implemented to be the DIC imaging system that can avoid the synchronization problem. Regarding the artery simulator, as reported previously [8], consists of a membrane pump, a PDMS phantom, and a computer for handling ECG signal generation and ECG signal detection. The membrane pump is used to draw water out of a tank and then the water is forced to go through the PDMS phantom with water pressure varied with the time; afterwards, the water will be sent back to the tank for completing the water circulating. A PDMS-made phantom is casted in a hollow cylindrical shape, whose height is 100 mm with \varnothing 50 mm and \varnothing 70 mm inner and outer diameter, a 4 mm diameter with 3 mm depth below the outer surface is cast to simulate a medium-size near-surface artery vessel inside an organ.

A computer-generated ECG signal drives the pump to allow the water pressure to vary with time. Then the water will go through the PDMS phantom intermittently to simulate the artery behaviors. Meanwhile, the generated ECG signal will also be injected back to the computer to detect the R-peaks and T-peaks for sending trigger signals to the camera for taking images. In the experiment, the computer-simulated ECG signal is first sent out to a DAQ; DAQ sends back the ECG signal to the computer to find the ECG R- and T-peaks. Then the triggering signal is sent out to activate the camera. That means, the single-camera stereo-DIC imaging system is used to capture images after the computer detects the ECG R-peaks and/or T-peaks. The time-lapse for imaging after the detection of R-peak/T-peak has been evaluated to be 15 ms [8].

In this study, the first taken R-peak image is always used as the reference image. Then two imaging operation modes are implemented to capture the operation images; the first mode is catching T-peak images after the first R-peak is detected; the second mode is continuously imaging immediately after the reference image is captured, as shown in Fig. 7.2. Regarding the time interval for continuously imaging is set to be 20 ms and the shutter time is 3 ms. Simultaneously, the membrane pump is derived by a home-made driver with the computer-generated ECG signal. The membrane pump is then intermittently drawing water out of a tank and then driving the water flow through the connecting vessels, the PDMS artery vessel phantom. It then flows back to the water tank to complete the water circulation through the system. The maximum volume of water the membrane pump can circulate is 400 ml/min. Considering the experiment is a dynamic case. Therefore, the exposure time is set to be a short one that is not good fluorescent practice and makes the measurement a great challenge. In this evaluation study, the VIC-3D of Correlated Solutions is used for displacement and strain calculation. The displacement and strain fields are described according to the coordinate system defined on the PDMS phantom, as shown in Fig. 7.3. The x-direction is normal to the direction of water flowing, and the y-direction is parallel to the inner vessel with the positive direction aligning to the water out. Meanwhile, in this study, the PDMS phantom is free placed with no strong fasten applied.

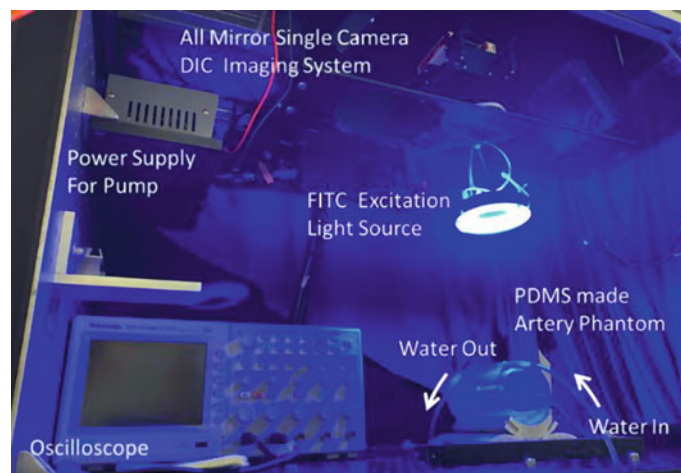


Fig. 7.1 Experimental Setup

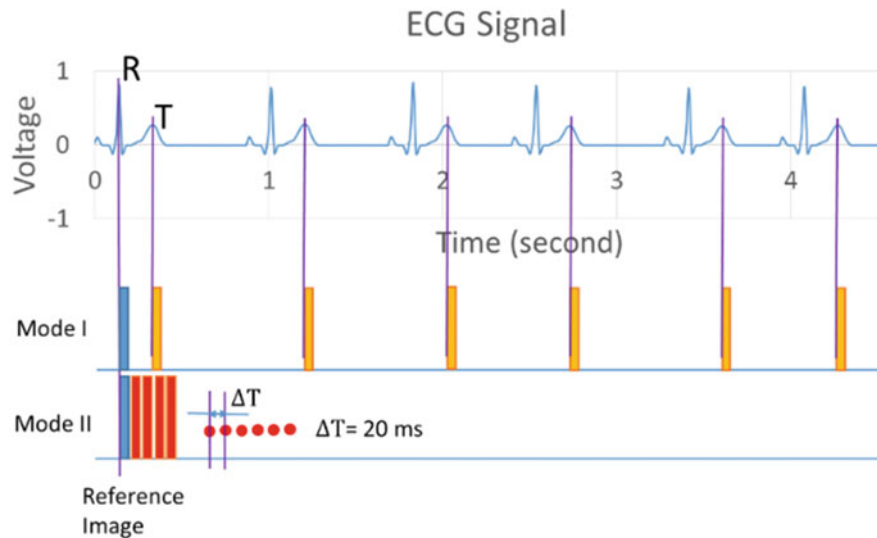
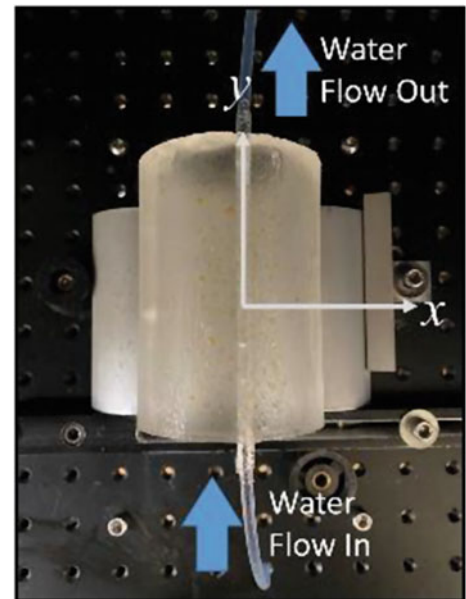


Fig. 7.2 Two imaging modes in this study

Fig. 7.3 PDMS phantom and the coordinate system



7.3 Results and Discussions

In this study, the FITC is first sprayed to the surface of the PDMS phantom; different from the typical applications of FITC on cells or tissues, the FITC emission light attenuates far more quick than the biomaterials. The random surface pattern does not last as long as the traditional paint spraying method; therefore, images taken by two image modes will have different surface artificial random patterns. The discussion on the displacement and strain field determined by two different imaging modes will not be quantitative but qualitative.

Figure 7.4 presents five selected displacement fields of the PDMS phantom as the images are continuously recorded after the first computer-generated ECG R-peak detected. From the averaged U-displacement plots, shown in Fig. 7.4a; the pumping water introduces the phantom to vibrate, and time-sequentially causes five specific displacement packages to the PDMS phantom, as shown inside the green-box of Fig. 7.4a, during the time the imaging system takes the first 180 images. Similar results can also be found at V- and W-averaged displacement plots; however, the V-displacement plot doesn't show the displacement packages as clear as the U- and W-averaged displacement plots. For U-displacement shown in Fig. 7.4a, although the averaged-displacements are different, the image frames #10 and # 25 have similar patterns. Those two

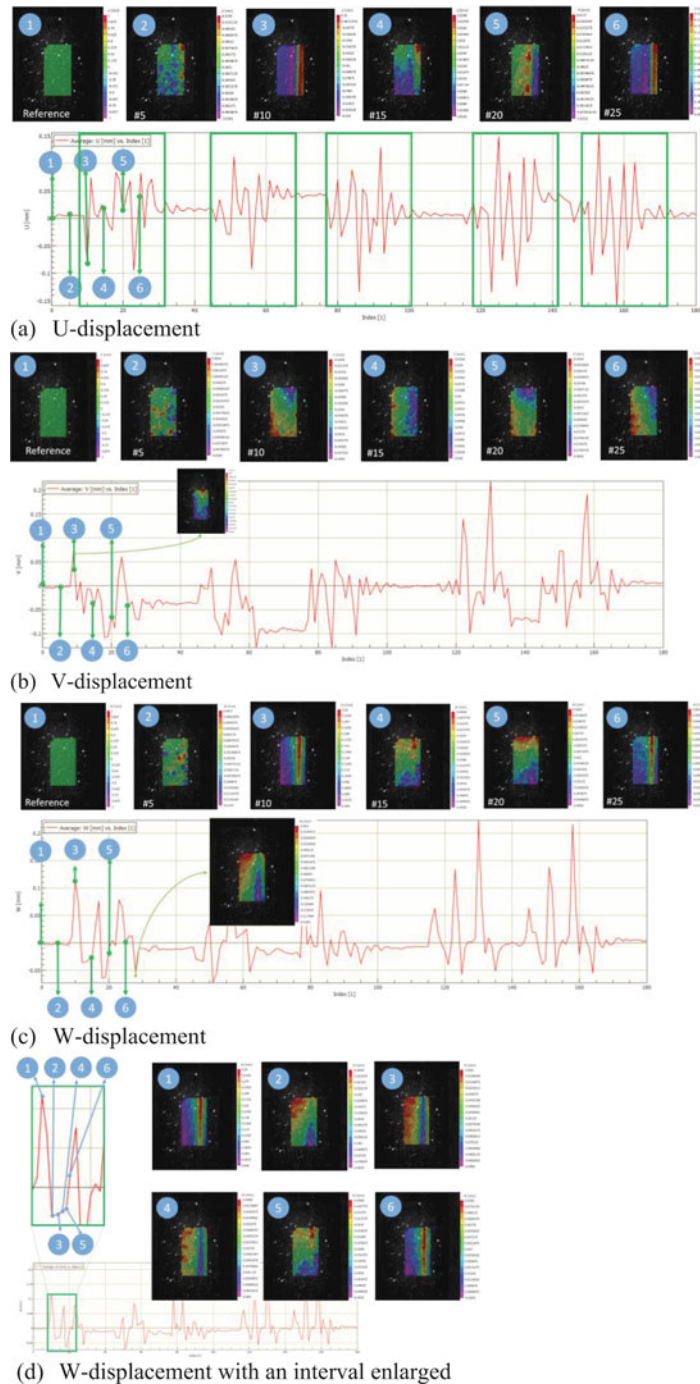


Fig. 7.4 The displacement field of the PDMS phantom subjected to water flow intermittently pumping through (a) U-displacement, (b) V-displacement, (c) W-displacement, (d) W-displacement with an interval enlarged

displacement fields show the right-hand side of the PDMS phantom inner vessel tends to move to the right and on the inner-vessel left-hand side tends to move to the left or less to the right; that means the surface of the inner vessel tends to expand. As for the V-displacement field shown in Fig. 7.4b, since the direction is parallel to the flow direction of the pumped water, without significant displacement, the results seem reasonable. However, while taking a close look at the top part of the PDMS, some remarkable local displacement can be observed, for example, images of frames #10, #20, and #25. Considering the region is of the same as the exit of the vessel to the connecting pipe. Therefore, the displacement would be regarded as introduced by the drag force. Regarding the W-displacement shown in Fig. 7.4c, image frames #10 and #25 reveal that the PDMS surface above the vessel tends to move upper; combining this observation with the U-displacement fields discussed

previously, it could easily be concluded that the water at these moments are pumping into the vessel. Besides, frames #15 and #20 also present local displacement around the inlet of the vessel. To understand this phenomenon, some of images between frames #15 and #20 are inspected with details; as shown in Fig. 7.4d, the interaction between intermittently pumping water and the PDMS phantom can be clearly observed from the series six frames. The water flowing into the vessel with relatively high pressure will cause the PDMS surface above the vessel to expand; then the water flows out and pumping pressure drops, then a local low-pressure region around the inlet of the vessel will build and extend to the exiting side of the vessel as the water flows out; after then, the volume of the vessel is no more fully filled with water; while the pump is active again, the water will be accelerated by pumping force and flow into the vessel to fill the space, then the inner pressure of the vessel would be increased rapidly.

Regarding the strain fields e_{yy} and e_{xy} , they do not present apparent patterns for the first 25 frames, as shown in Fig. 7.5b, c. However, e_{xy} shows a very interesting local strain at the middle of the vessel, but no proper physical model can adequately

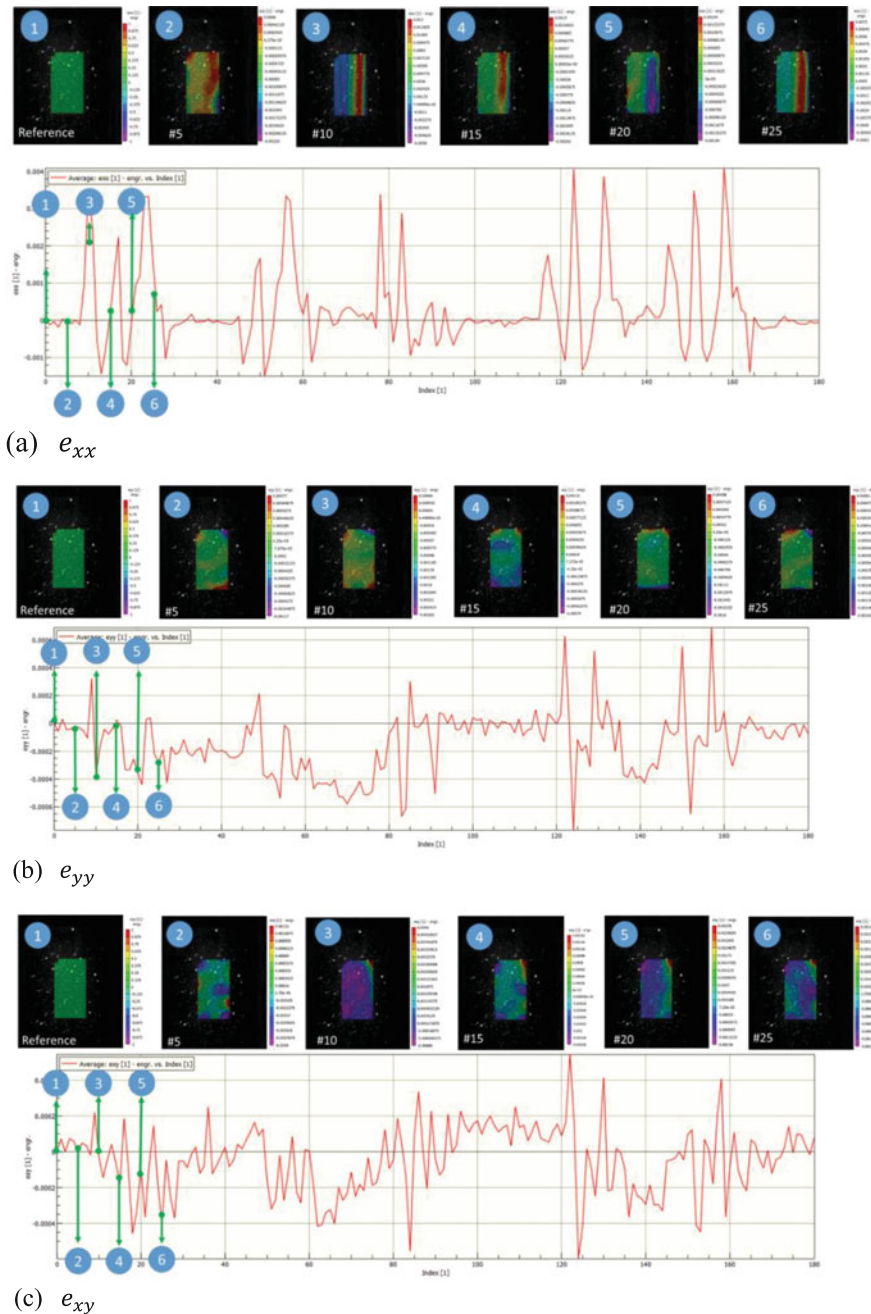


Fig. 7.5 The strain field of the PDMS phantom subjected to water flow intermittently pumping through (a) e_{xx} , (b) e_{yy} , (c) e_{xy}

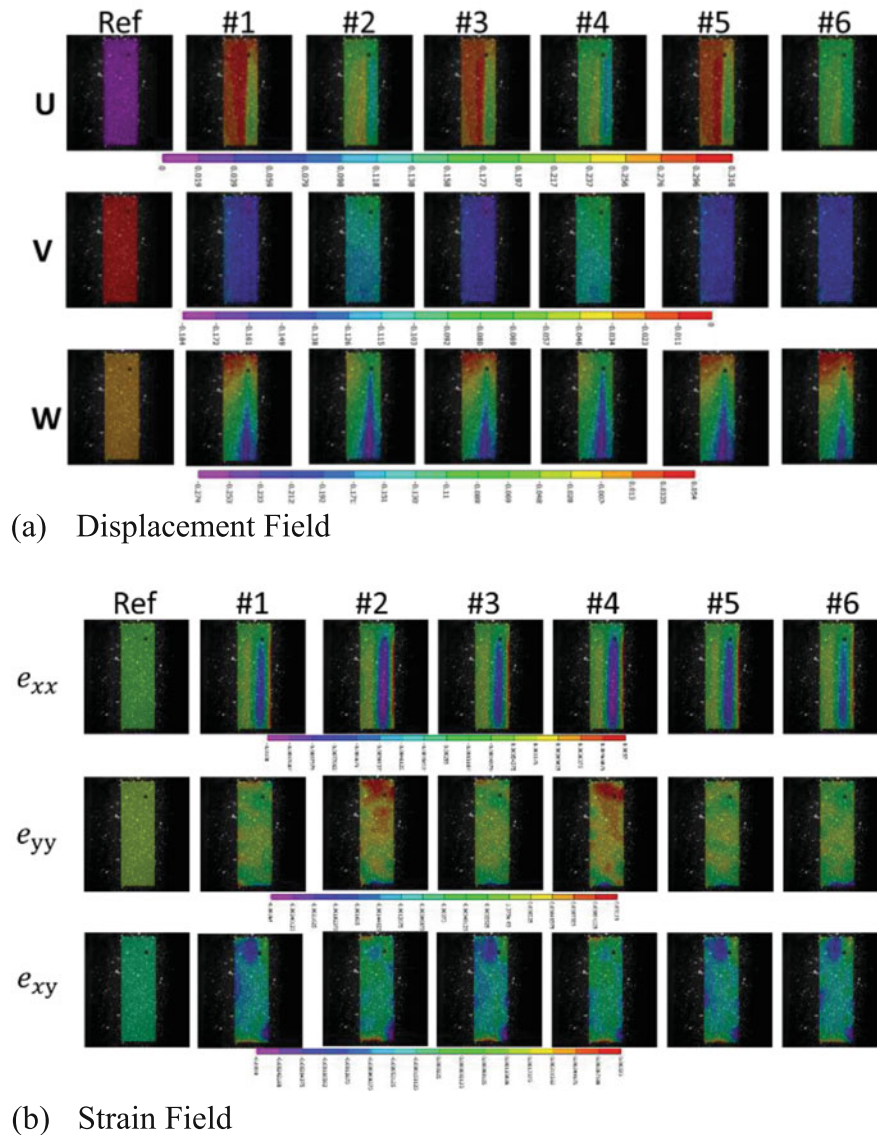


Fig. 7.6 The displacement and strain field of the PDMS phantom subjected to water flow intermittently pumping through (a) displacement field, (b) strain field

explain this strain field. Based on the displacement field discussed previously, the U-displacement fields shown in frame #10 and #25 indicate the surface of PDMS above the vessel tends to expand; intuitively, the strain fields e_{xx} of those two frames are expansive strain as shown in Fig. 7.5a. Aside from the previous results, frame #20 of Fig. 7.5a shows a compressive strain field above the vessel that is not observed from the corresponding U-displacement field shown in Fig. 7.4a; obviously, the strain field e_{xx} provides more data, sensitive, than the U-displacement field.

The other imaging mode is taking the first image as reference one while the ECG R-peak is detected. Then the imaging system continuously takes images as ECG T-peaks caught. The fetched images are then used for displacement and strain calculation by the DIC method. The calculated strain and displacement fields are presented in Fig. 7.6a and Fig. 7.6b, respectively. Different from the previous results, the displacement and strain fields here are repeatedly calculated as T-peaks detected. Therefore, if the ECG signal is correctly repeated and the output power of the pump is well controlled, then the resulting displacement and strain would be almost the same; that means this image mode can be used to evaluate how stable the simulator is. As shown in Fig. 7.6, the displacement and strain fields can be divided into two groups. For the first group, the displacement and strain fields of #1, #3, and #5 T-peaks are almost identical, as for the other group is the displacement and strain field determined using the images taken as #2 and #5 T-peaks detected. Even though the displacement and strain fields

seem can be divided into two groups, the displacement and strain magnitudes are not varied tremendously. Based on the resulted displacement and strain field, a small output performance variation existing in the simulator can be evaluated. Still, the influence on the mechanical interactions between the PDMS and the water introduced by the variation of the simulator is limited.

Regarding the displacement field conducted by the PDMS-water interaction, the U-displacement indicates the PDMS tends to move to the right. The region above the vessel tends to shrink because the U-displacement on the right-hand side above the vessel is smaller than the displacement magnitude of the left-hand side. As for the V-displacement, the plots show that the PDMS would be uniformly moved towards the connecting pipe on the inlet side; however, the physical model for explaining the displacement is not available now. From the W-displacement field, the region above the vessel tends to move down at the inlet side and tends to move up at the exit side; this indicates pressure inside the vessel dropped near the inlet side and the whole PDMS is left up at the exit side. The displacement indicates pressure inside the vessel dropped at the inlet side and then causes the surface above the vessel move downwards. As for the exit end, the displacement might be caused by superposing a local expansion and a vibration. Regarding the local expansion, since the diameter of connecting pipe is smaller than the through hole of PDMS (to simulate the vessel), the inner pressure of the vessel is locally high and might cause the region around the exit side to expand.

The strain fields are present in Fig. 7.6b, the e_{xx} of all six successive frames show the normal strain above the PDMS vessel are all in compressive, and the magnitudes are highest at frames #2 and #4. Regarding the strain field e_{yy} , frames #1, #3, #5, and #6 show that most of the PDMS phantom is subjected to small compressive strain but relatively small extensive strain in the other regions. The PDMS upper part shows a relatively high extension strain value for e_{yy} of the #2 and #4 frames. Besides, while inspecting Fig. 7.6b with care, the strain field around the inlet and exit edges shows a small compressive and extensive e_{yy} , respectively; the strain e_{yy} around the edge might be caused by the pressure drop at the inlet, and the high pressure introduced by diameter mismatch at the outlet side. Regarding the shear strain e_{xy} , frames #1, #3, #5, and #6 indicate the upper-left, and bottom-right of the vessel are subjected to the shear strain locally but different sign. Similar results can be observed from frames #2 and #4; however, the shear strains at the upper-left part are relatively small compared with the other cases. More interest, when the e_{xy} is relatively uniform, the e_{xx} above the vessel apparent more strong compressive strain.

From the above discussion, the developed artery vessel simulator can provide relatively stable mechanical behaviors at each T-peak from the above discussion. The time-sequential mechanical behaviors are varied for the V-displacement, e_{yy} , and e_{xy} .

In this study, the developed artery-vessel simulator is deeply investigated using a self-developed single-camera stereo-DIC system. The random surface pattern of the artery-vessel simulator is prepared using FITC. FITC is a fluorescent substance that has been widely used for cell and tissue studies. Typically the FITC is prepared by dissolving the powder with water. In this study, the FITC is sprayed on the surface of PDMS to provide a random pattern for tracking; however, the water will evaporate rapidly if the size of the drop is small. And then the emitting light will attenuate. In contrast, the drop will move due to the self-weight of the drop is large; the drop will also move while subjected to the force as the water intermittently flow through the PDMS that will introduce the pattern changed. Therefore, different from the traditional artificial random pattern, the FITC random pattern cannot last as long as the random pattern generated with ink and paint. Although many fluorescent medicines can be used to generate random patterns for DIC use, more works are required for handling the problem mentioned.

7.4 Conclusions

In this study, FITC is used to generate the random pattern on the PDMS surface. Then the random patterns are tracked from frame to frame using the DIC algorithm for evaluating the associated displacement and strain among frames for evaluating the mechanical behaviors of the proposed artery-vessel simulator. The proposed simulator has proved to be relatively stable for simulating the mechanical behaviors among the first detected ECG R-peak and the following T-peaks. As for time-sequential mechanical behaviors, the simulator might need additional adjustment to make the mechanical behaviors more consistent. Although the FITC can be used for DIC application, the emitting light attenuation because of the water evaporation needs to be solved.

Acknowledgments This paper was supported in part by the Ministry of Science and Technology, Taiwan (Grand no. MOST-107-2221-E-492-012 and MOST-108-2221-E-492-022-MY2).

References

1. Berfield, T.A., et al.: Fluorescent image correlation for nanoscale deformation measurements. *Small*. **2**(5), 631–635 (2006)
2. Praveen, G.B., Raghavendra, S., Chang, V.I.C.: An analysis of leg muscle stretch using 3D digital image correlation. *Int J Organiz Collective Intell*. **7**(3), 30–43 (2017)
3. Xue, Y., et al.: High-accuracy and real-time 3D positioning, tracking system for medical imaging applications based on 3D digital image correlation. *Opt. Lasers Eng*. **88**, 82–90 (2017)
4. Solav, D., et al.: MultiDIC: an open-source toolbox for multi-view 3D digital image correlation. *IEEE Access*. **6**, 30520–30535 (2018)
5. Hokka, M., et al.: In-vivo deformation measurements of the human heart by 3D digital image correlation. *J. Biomech*. **48**(10), 2217–2220 (2015)
6. Hokka, M., et al.: DIC Measurements of the human heart during cardiopulmonary bypass surgery. In: *Mechanics of Biological Systems and Materials*, pp. 51–59. Springer, Cham (2016)
7. Soltani, A., et al.: An optical method for the in-vivo characterization of the biomechanical response of the right ventricle. *Sci. Rep*. **8**(1), 1–11 (2018)
8. Hwang, C.-H., et al.: Evaluating the application of DIC on heartbeat detection by using a self-developed artery vessel simulator, *Mechanics of Biological Systems & Micro-and Nanomechanics, Volume 5 of the Proceedings of the 2020 SEM Annual Conference & Exposition on Experimental and Applied Mechanics* (2021)